Published in final edited form as:
Science. 2013 January 25; 339(6118): . doi:10.1126/science.1228360.

An Actin-Dependent Step in Mitochondrial Fission Mediated by the ER-Associated Formin INF2

Farida Korobova[1], **Vinay Ramabhadran**[2], and **Henry N. Higgs**[1,*]

[1]Department of Biochemistry, Geisel School of Medicine at Dartmouth, Hanover, NH 03755, USA

[2]Howard Hughes Medical Institute, Sackler School of Graduate Biomedical Sciences, Tufts University, Boston, MA 02111, USA

Abstract

Mitochondrial fission is fundamentally important to cellular physiology. The dynamin-related protein Drp1 mediates fission, and interaction between mitochondrion and endoplasmic reticulum (ER) enhances fission. However, the mechanism for Drp1 recruitment to mitochondria is unclear, although previous results implicate actin involvement. Here, we found that actin polymerization through ER-localized inverted formin 2 (INF2) was required for efficient mitochondrial fission in mammalian cells. INF2 functioned upstream of Drp1. Actin filaments appeared to accumulate between mitochondria and INF2-enriched ER membranes at constriction sites. Thus, INF2-induced actin filaments may drive initial mitochondrial constriction, which allows Drp1-driven secondary constriction. Because INF2 mutations can lead to Charcot-Marie-Tooth disease, our results provide a potential cellular mechanism for this disease state.

Mitochondrial function extends far beyond that of energy generation, because mitochondria act as sensors of metabolic homeostasis and are key players in cell death pathways (1–4). The dynamic ability of mitochondria to undergo fission and fusion and to move in cells is important for mitochondrial function, and defects in mitochondrial dynamics are implicated in many neurodegenerative diseases (5, 6). Fission involves oligomerization of dynamin-related protein 1 (Drp1, called Dnm1 in yeast) into a helical ring around the outer mitochondrial membrane, followed by ring constriction. The mechanism for Drp1 recruitment to fission sites, however, is unclear. The diameter of the Drp1 ring is narrower (100 to 130 nm for Dnm1) than an unconstricted mitochondrion (7), which suggests that prior constriction may be required. Mitochondrial fission occurs preferentially at endoplasmic reticulum (ER) contact sites, with ER circumscribing mitochondria (8). Mitochondria are constricted at these ER contact sites even when Drp1 activity is compromised (8). Drp1- and Dnm1-independent constriction is also observed in *Caenorhabditis elegans* (9) and budding yeast (10), respectively. The mechanism of Drp1-independent mitochondrial constriction is unknown, although actin filaments are implicated in the process (11).

*To whom correspondence should be addressed. henry.higgs@dartmouth.edu.

Supplementary Materials
www.sciencemag.org/cgi/content/full/339/6118/464/DC1
Materials and Methods
Figs. S1 to S10
References
Movies S1 to S6

Inverted formin 2 (INF2) is a vertebrate formin protein that accelerates both actin polymerization and depolymerization (12). In mammalian cells, INF2 exists as two isoforms differing in C-terminal sequence (fig. S1): the prenylated (CAAX) isoform, which is tightly bound to ER (13), and the nonCAAX isoform, which is cytoplasmic (14). Suppression of INF2-nonCAAX in tissue culture cells causes Golgi dispersal (14). In contrast, the cellular function of INF2-CAAX is unclear because its suppression has no apparent effect on ER structure or dynamics (13). Physiologically, mutations in INF2 are linked to two human diseases: focal and segmental glomerulosclerosis, a degenerative kidney disease (15), and Charcot-Marie-Tooth disease (CMTD), a peripheral neuropathy (16).

We decided to test a role for INF2 in controlling mitochondrial size, on the basis of two factors. First, mitochondrial fission takes place at ER contact sites (8). Second, other proteins mutated in CMTD affect mitochondrial dynamics (17–19). INF2 suppression by small interfering RNAs (siRNAs) in either a human osteosarcoma cell line (U2OS) (Fig. 1, A and B, and fig. S2C) or a mouse fibroblast line (NIH 3T3) (fig. S2, A and B) resulted in significant increases in mitochondrial average length and in the percentage of mitochondria over 5 μm. We then tested whether specific suppression of INF2-CAAX in U2OS cells would result in similar mitochondrial elongation. When we treated U2OS cells with two distinct siRNAs that specifically suppressed INF2-CAAX (fig. S3), mitochondrial length increased 2.5 times (Fig. 1, A and B). However, INF2-CAAX depletion did not cause Golgi expansion (fig. S4), an effect attributable to INF2-nonCAAX (14). U2OS cells express considerably less INF2-CAAX than NIH 3T3 cells (14) but did express detectable levels of INF2-CAAX protein (fig. S3B). Thus, suppression of INF2-CAAX, which localizes to ER, causes an increase in mitochondrial length.

We then tested whether INF2-CAAX overexpression would induce an effect on mitochondria opposite to INF2-CAAX suppression. A green fluorescent protein (GFP)–fusion construct of INF2-CAAX wild type (INF2-WT) localized to ER in U2OS cells (14). However, this construct did not cause a significant change in mitochondrial length (Fig. 2, A and B). We reasoned that INF2-WT might be autoinhibited, because INF2 has autoinhibitory sequences similar to other formins (13). To test this hypothesis, we changed Ala^{149} to aspartic acid (D), because a similar mutation in the formin mDia1 causes constitutive activation (20). INF2-A149D decreased mitochondrial length by a factor of 2.2 (Fig. 2, A and B). In addition, INF2-A149D cells displayed a higher frequency of constricted ER-mitochondrial contact sites than control cells (Fig. 2C and fig. S5D). Thus, constitutively active INF2-CAAX causes a decrease in mitochondrial length and an increase in mitochondrial constriction frequency.

We examined INF2-A149D effects in more detail by live-cell microscopy, using ER-green [ER-targeting sequence of ubiquitin-conjugating enzyme E2 6 (UBC6) fused to GFP (21)] as a negative control. In ER-green cells, infrequent fission events occurred (fig. S5A and movie S1). In contrast, fission events were about three times as frequent in INF2-A149D cells (fig. S5, B and C). These fission events always corresponded to regions where INF2 circumscribed the mitochondrion (Fig. 2D and movie S2). In addition, mitochondria were less mobile in INF2-A149D cells than in ER-green or INF2-WT cells (Fig. 2E, fig. S6, and movies S3 to S6).

The decrease in mitochondrial mobility raised the possibility that INF2's effect on mitochondrial size was due to an indirect effect on fusion, because it prevented mitochondria from interacting. Indeed, quantification of live-cell images indicated a decrease by a factor of 2.3 in mitochondrial fusion in INF2-A149D cells (fig. S5, B and C). Thus, INF2-A149D results in both an increase in fission and a decrease in fusion. However, analysis of live-cell images of INF2-suppressed cells revealed a drop by a factor of 2.2 in

fission events with only a minor decrease in fusion (fig. S5, B and C). Thus, we conclude that INF2 has a direct effect on mitochondrial fission, whereas the effect of INF2-A149D on fusion is indirect, owing to a decrease in mitochondrial mobility.

Because Drp1 acts in mitochondrial fission, we examined a potential connection between INF2 and Drp1. Drp1 localized to cytoplasm and to mitochondrially associated puncta in U2OS cells (Fig. 3, A and C). Suppression of Drp1 reduced mitochondrially associated puncta, in addition to causing mitochondrial elongation (Fig. 3A and fig. S7, A and B). Drp1 puncta also decreased upon INF2 suppression (Fig. 3, A and B), without a reduction in total cellular Drp1 (fig. S7A). In contrast, INF2-A149D expression caused dense Drp1 puncta associated with mitochondria (Fig. 3D). Thus, INF2 facilitates interaction of Drp1 with mitochondria. If Drp1 acts downstream of INF2, alterations in Drp1 activity should inhibit INF2-A149D–induced mitochondrial fission. Both Drp1 suppression by siRNA and the dominant-negative (guanosine triphosphatase–deficient) K38E Drp1 construct (in which Glu replaces Lys^{38}) reversed the effect of INF2-A149D on mitochondria size, with the K38E mutant producing a stronger effect (Fig. 3. E and F). Thus, INF2-mediated mitochondrial fission occurs through Drp1.

The fact that Drp1 suppression resulted in longer average mitochondria than did INF2 suppression (fig. S7B and Fig. 1B) might be due to several factors that are not mutually exclusive. First, INF2 may only participate in a subset of fission reactions. Second, INF2 activity may not be essential for fission but may facilitate the process. Third, low levels of INF2-CAAX may be sufficient to mediate fission, such that RNA interference–mediated suppression is insufficient for full inhibition.

INF2 interacts with both actin and microtubules (22), and its effects on mitochondria could be mediated through either cytoskeletal element. We used the actin monomer–sequestering drug latrunculin B (LatB) to test a role for actin in mitochondrial fission. LatB significantly increased mitochondrial length in U2OS cells (Fig. 4, A and B), similar to its effect on other cell types (11). Furthermore, LatB antagonized INF2-A149D–induced mitochondrial shortening (Fig. 4, A and B). To test further the relevance of actin filaments to INF2's mitochondrial effects, we mutated a key actin polymerization residue, Ile^{643} (fig. S1) (23). The I643A mutation antagonized the effects of INF2-A149D on both mitochondrial length and mitochondrial mobility (Fig. 2 and movie S6). This mutation did not alter INF2-microtubule interactions (fig. S8), which indicated that its effects were specific to actin regulation. Thus, INF2 affects mitochondrial length and ER-mitochondrial interaction in an actin-dependent manner.

We sought direct evidence for actin filament accumulation at ER-mitochondrial contact sites, using laser scanning confocal microscopy to construct three-dimensional (3D) images. This analysis was difficult because of the abundance of stress fibers and other cytoplasmic actin filaments, which obscured potential mitochondrially associated actin. Analysis of U2OS cells transfected with INF2-WT revealed filament accumulation at 16% of ER-mitochondrial contact sites (fig. S9, B and C). Cells transfected with INF2-A149D displayed a higher percentage (65%) of actin-enriched ER-mitochondrial contacts (Fig. 4, C to E, and fig. S9, A and C), with peak filament staining occurring between the mitochondrial and INF2 staining (Fig. 4E). Thus, actin can polymerize at the ER-mitochondrial interface during constriction and/or fission. We postulate that actin is not observable at every ER-mitochondrial contact because these filaments are transient, as they may be both polymerized and depolymerized by INF2. It is also possible that actin polymerization is required for only a subset of fission events. Such heterogeneity is consistent with the variety of Drp1 isoforms, adaptors, and posttranslational modifications associated with mammalian mitochondrial fission (24).

We suggest a potential mechanism explaining the finding that ER association stimulates mitochondrial fission (8) (fig. S10). At the mitochondria-ER interaction site, INF2 is activated to polymerize actin. Actin polymerization between ER and mitochondrion could possibly enable force generation to drive initial mitochondrial constriction and to enhance Drp1 ring assembly at the constriction site. Drp1 activity further constricts the mitochondrion, which results in fission. INF2's severing and/or depolymerization activity could rapidly remove actin filaments after fission. Force could be generated directly through actin polymerization or through myosin motor activity (25). This model supports previous findings suggesting that Drp1 oligomeric rings are narrower than unconstricted mitochondria (7) and that mitochondria can constrict in a Drp1-independent manner (8–10).

Supplementary Material

Refer to Web version on PubMed Central for supplementary material.

Acknowledgments

We thank M. Zick, J. Moseley, B. Wickner, and C. Barlowe for useful discussions; A. Lavanway for help with the microscopes; and M. Richio-Dalton for her tireless energy. Portions of this publication are covered in a pending patent application. "Methods for modulating mitochondrial function via INF2," H. Higgs author, Patent DC512US.L. Supported by NIH grants GM069818 and DK88826 to H.N.H. Funds to purchase the Nikon A1RSi confocal workstation were provided by NSF award DBI1039423.

References and Notes

1. Nunnari J, Suomalainen A. Cell. 2012; 148:1145. [PubMed: 22424226]
2. Martinou JC, Youle RJ. Dev Cell. 2011; 21:92. [PubMed: 21763611]
3. Hoppins S, Nunnari J. Science. 2012; 337:1052. [PubMed: 22936767]
4. Youle RJ, van der Bliek AM. Science. 2012; 337:1062. [PubMed: 22936770]
5. Chen H, Chan DC. Hum Mol Genet. 2009; 18(R2):R169. [PubMed: 19808793]
6. Correia SC, et al. Adv Exp Med Biol. 2012; 724:205. [PubMed: 22411245]
7. Mears JA, et al. Nat Struct Mol Biol. 2011; 18:20. [PubMed: 21170049]
8. Friedman JR, et al. Science. 2011; 334:358. [PubMed: 21885730]
9. Labrousse AM, Zappaterra MD, Rube DA, van der Bliek AM. Mol Cell. 1999; 4:815. [PubMed: 10619028]
10. Legesse-Miller A, Massol RH, Kirchhausen T. Mol Biol Cell. 2003; 14:1953. [PubMed: 12802067]
11. De Vos KJ, Allan VJ, Grierson AJ, Sheetz MP. Curr Biol. 2005; 15:678. [PubMed: 15823542]
12. Chhabra ES, Higgs HN. J Biol Chem. 2006; 281:26754. [PubMed: 16818491]
13. Chhabra ES, Ramabhadran V, Gerber SA, Higgs HN. J Cell Sci. 2009; 122:1430. [PubMed: 19366733]
14. Ramabhadran V, Korobova F, Rahme GJ, Higgs HN. Mol Biol Cell. 2011; 22:4822. [PubMed: 21998196]
15. Brown EJ, et al. Nat Genet. 2010; 42:72. [PubMed: 20023659]
16. Boyer O, et al. N Engl J Med. 2011; 365:2377. [PubMed: 22187985]
17. Cartoni R, Martinou JC. Exp Neurol. 2009; 218:268. [PubMed: 19427854]
18. Niemann A, Ruegg M, La Padula V, Schenone A, Suter U. J Cell Biol. 2005; 170:1067. [PubMed: 16172208]
19. Vital A, et al. Neuromuscul Disord. 2012; 22:735. [PubMed: 22546700]
20. Otomo T, Otomo C, Tomchick DR, Machius M, Rosen MK. Mol Cell. 2005; 18:273. [PubMed: 15866170]
21. WoŸniak MJ, et al. J Cell Sci. 2009; 122:1979. [PubMed: 19454478]
22. Gaillard J, et al. Mol Biol Cell. 2011; 22:4575. [PubMed: 21998204]

23. Ramabhadran V, Gurel PS, Higgs HN. J Biol Chem. 2012; 287:34234. [PubMed: 22879592]
24. Elgass K, Pakay J, Ryan MT, Palmer CS. Biochim Biophys Acta. 2013; 1833:150. [PubMed: 22580041]
25. DuBoff B, Götz J, Feany MB. Neuron. 2012; 75:618. [PubMed: 22920254]

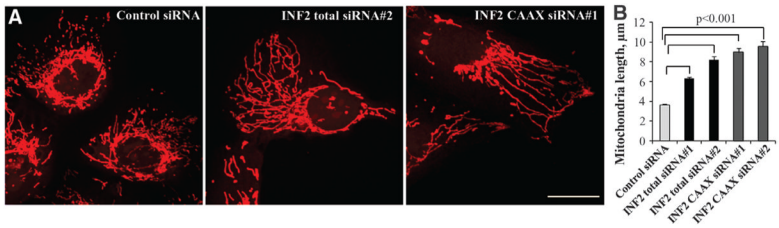

Fig. 1.

INF2 suppression increases mitochondrial length. (**A**) Maximum intensity projections of confocal images of MitoTracker-labeled U2OS cells treated with the indicated siRNAs. Scale bar, 20 μm. (**B**) Quantification of mitochondrial lengths. n = 157 to 531 mitochondria. Error bars, SEM.

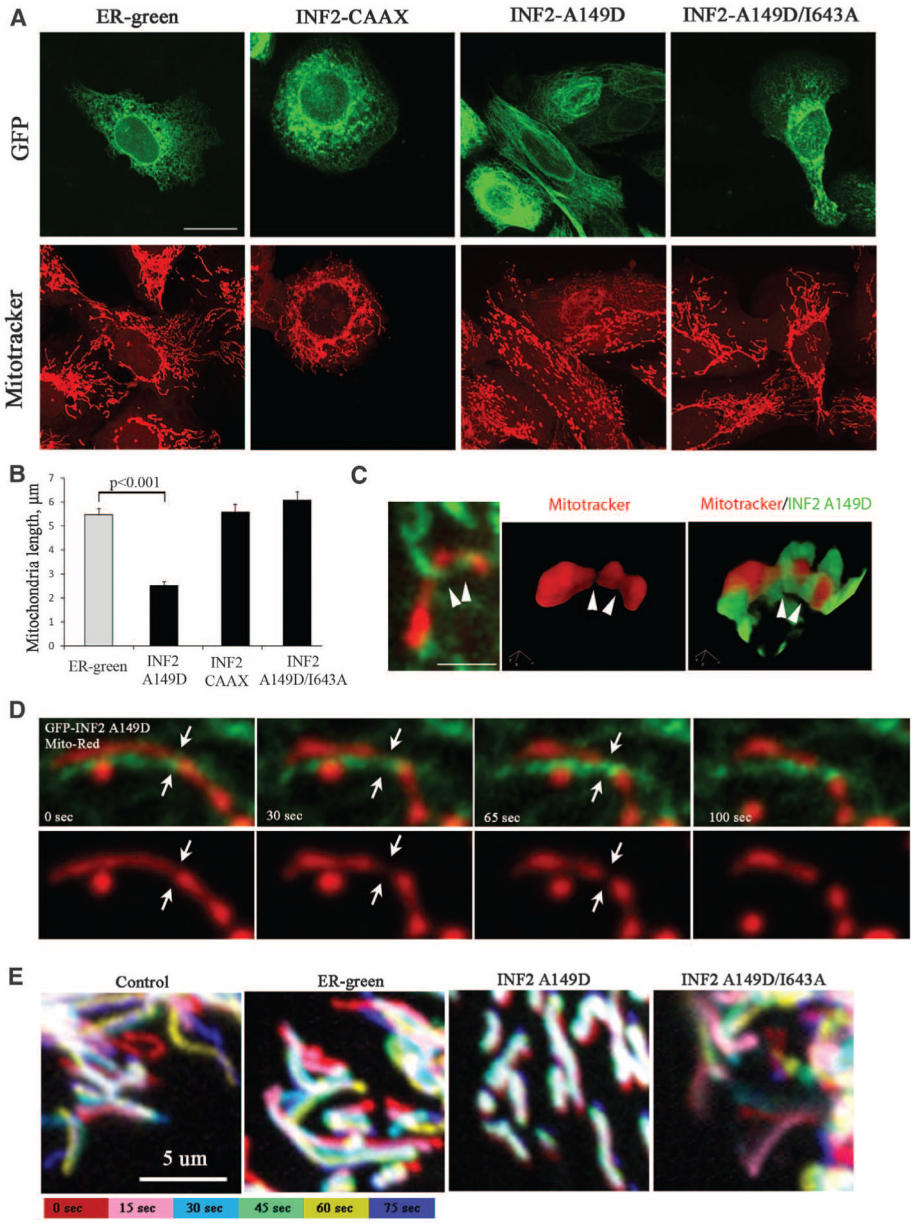

Fig. 2.

Constitutively active INF2-CAAX decreases mitochondrial length and dynamics. (**A**) Micrographs of U2OS cells transfected with GFP-fusions and labeled with MitoTracker. INF2 constructs are CAAX. Scale bar, 20 μm. (**B**) Quantifications of mitochondrial length. *n* = 158 to 537 mitochondria. Error bars, SEM. (**C**) Confocal micrographs of mitochondrion in close association with INF2-A149D. (Left) Maximum intensity projection of z stack. (Right) 3D reconstruction of MitoTracker alone or MitoTracker with GFP overlay. Arrowheads indicate constriction and/or fission sites. Scale bar, 2 μm. (**D**) Mitochondrial dynamics (mitochondria labeled using Mito Red) in U2OS transfected with GFP–INF2-A149D. Arrows indicate the fission event. Scale bar, 5 μm. (**E**) Overlays of mitochondrial dynamics time course in cells transfected with indicated constructs. Colors depict time points in the sequence, with white color indicating relative immobility.

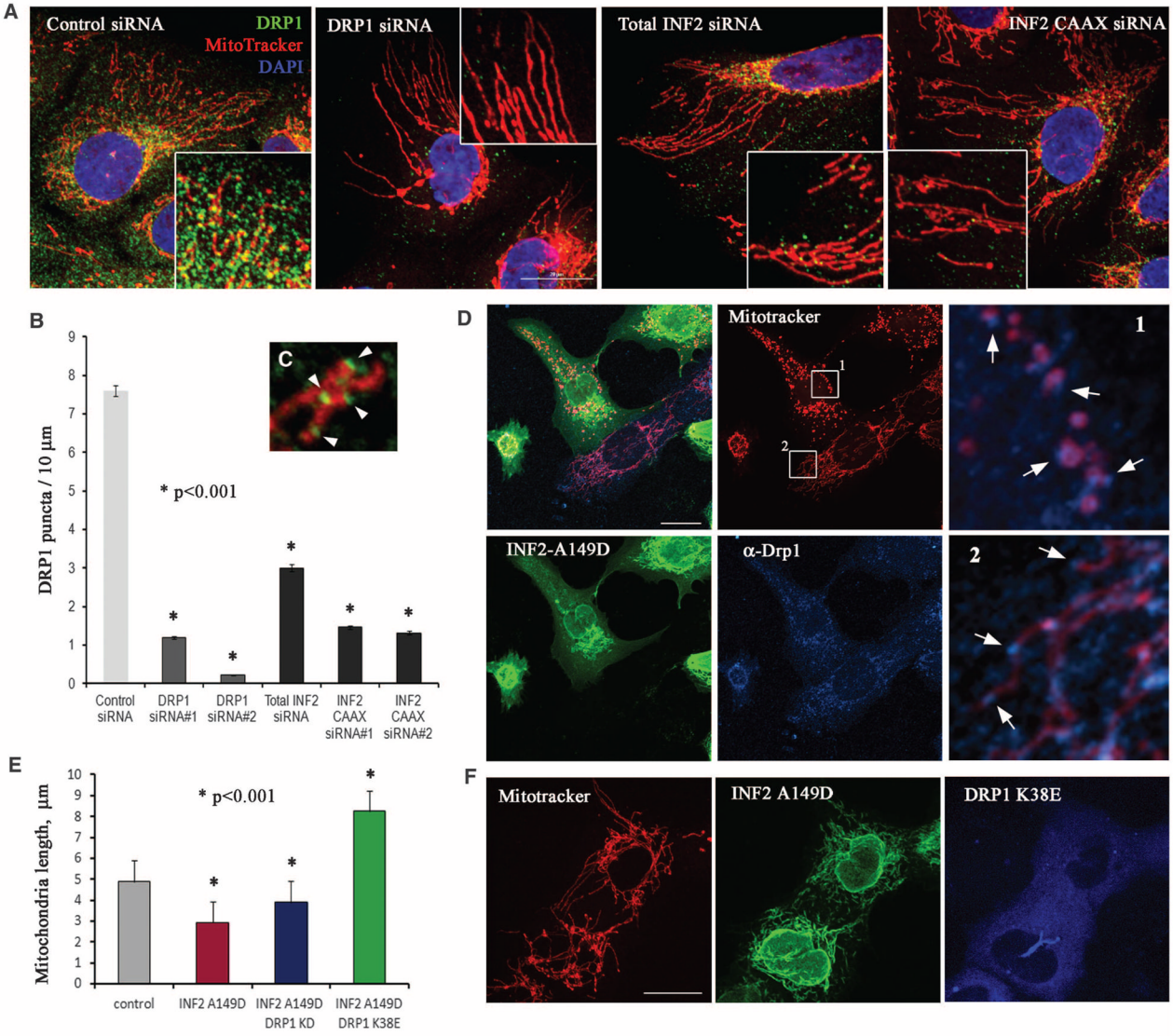

Fig. 3.

INF2 enhances Drp1-mitochondria association. (**A**) Confocal micrographs of U2OS cells labeled with an antibody against Drp1 (green) after indicated siRNA treatment. MitoTracker staining (red), and 4′,6-diamidino-2-phenylindole (DAPI) staining (blue). (Insets) Close-ups of peripheral cellular regions. Scale bar, 20 μm. (**B**) Quantification of Drp1 puncta per mitochondrial length, $n = 40$ to 68 mitochondria. Error bars, SEM. (**C**) Example of Drp1 puncta localization to mitochondria (arrowheads). (**D**) Effect of INF2-A149D expression (green) on Drp1 puncta. Mitochondria (red), Drp1 (blue). (Right) Close-ups of regions in INF2-A149D (1) and control cells (2). Scale bar, 20 μm. (**E** and **F**) Inhibition of Drp1 reduces the effect of INF2-A149D and makes mitochondria longer. (E) Quantification of mitochondrial length upon INF2-A149D expression and either Drp1 suppression or Drp1 K38E coexpression. $n = 199$ to 531 mitochondria. Error bars, SEM. (F) Confocal micrographs of U2OS cells coexpressing Mito Red (red), INF2-A149D (green), and Drp1 K38E (blue). Scale bar, 20 μm.

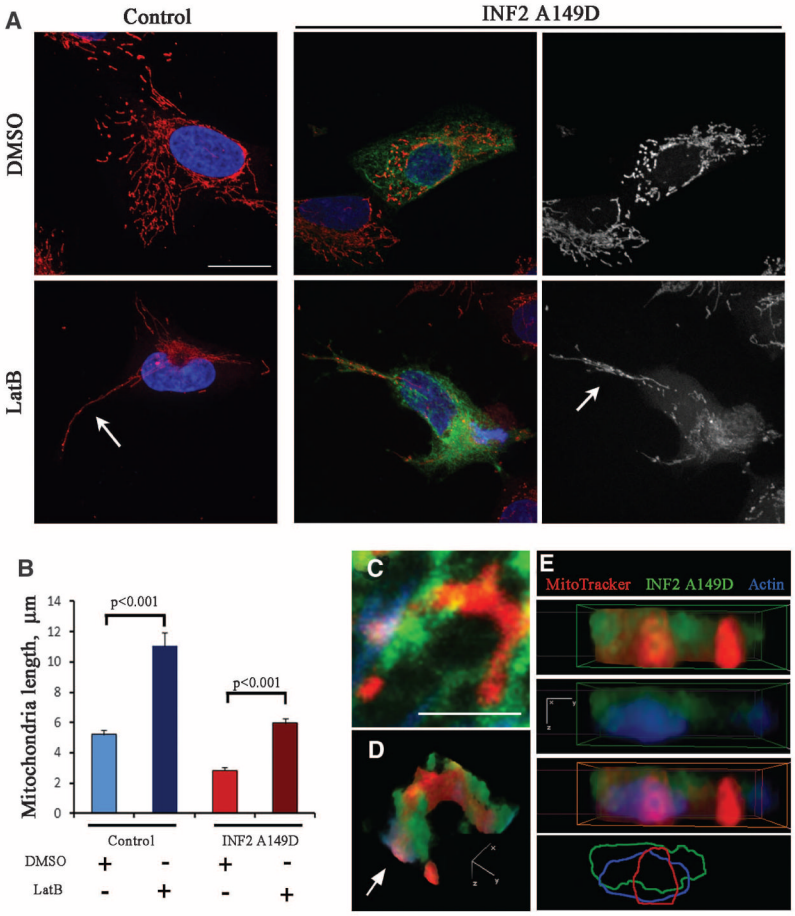

Fig. 4.

Actin filaments are required for INF2-mediated mitochondrial fission. (**A**) Control or INF2-A149D U2OS cells treated with dimethyl sulfoxide (DMSO) or 0.5 µM LatB for 60 min. Maximum intensity projections of six to nine z steps. Scale bar, 20 µm. Arrows indicate long mitochondria. (**B**) Quantification of mitochondrial lengths after DMSO or LatB. $n = 53$ to 110 mitochondria. Error bars, SD. (**C** to **E**) 3D reconstruction of mitochondrion (red) in INF2-A149D cell (green) labeled with Alexa660-phalloidin (blue). (C) Maximum intensity projection of nine z steps (D) Volume rendering of (C). (E) Same mitochondrion viewed along *x* axis [arrow in (D)], presented as 3D combinations. (Bottom) Outlines of stains to illustrate relative positions. Scale bar, 2 µm.